JOURNAL OF MATERIALS SCIENCE 28 (1993) 4583–4594

Influence of reactant characteristics on the microstructures of combustion-synthesized titanium carbide

D. C. HALVERSON*, K. H. EWALD, Z. A. MUNIR
Division of Materials Science and Engineering, College of Engineering, University of California, Davis, CA 95616, USA

The influence of reactant characteristics on morphological development through the stages of combustion synthesis was investigated using a titanium–carbon system. The effect of the characteristics of a variety of carbons (carbon blacks, graphites, and cokes) and a variety of titanium powders on the density and microstructure of combusted and uncombusted sample compacts was studied. The size of the titanium particles had a relatively small influence on the density of the final (TiC) product but had a significant effect on its microstructure. The structure of the carbon blacks (as judged by the n-dibutyl phthalate absorption number, DBP) had a direct influence on the density of the uncombusted and combusted samples: low-structure carbon blacks resulted in higher densities for both cases. Products made with natural graphites had higher densities than those made with synthetic graphites. The surface area of carbon and graphite reactant powders had less influence on the density of the product than on its network morphology. Cored structures in TiC products made from certain carbon and graphite powders were observed and are explained in terms of their ash (oxide) content.

1. Introduction

In the field of combustion synthesis a great deal of emphasis has been placed on the need to produce fully dense materials. Less attention has been given to this process as a method for the preparation of porous ceramic bodies to be used as filters or as preforms for molten metal or polymer infiltration. The feasibility of synthesizing bodies with 40–60% porosity is an intrinsic feature of combustion synthesis and as such offers the potential for the fabrication of ceramic–polymer, metal–matrix, and ceramic–metal composites.

The lack of attention paid to this aspect of combustion synthesis has resulted in a deficiency in our understanding of how pre-combustion variables relate to post-combustion microstructures of the products. This work represents the first in a series of articles that address this issue [1]. This paper reports the influence of the reactants' physical and chemical properties on the uncombusted and combusted sample densities and microstructures. The specific system investigated in this work is the synthesis of TiC through an exothermic reaction between carbon and titanium.

2. Experimental procedures

2.1. Reactants and their characterization

The titanium powders used in this study were obtained from five suppliers. The characteristics of these powders and their chemical analyses are given in Table I. X-ray diffraction (XRD) analysis showed trace amounts of TiC in the Alfa 00724 powder, TiO and Ti_2N in the Ventron Grade-Z powder, TiC in the Micron Ti-020 powder, TiC, TiO, and Ti_2N in the Atlantic-325 mesh powder, and TiH_2 in the Alfa 99883 powder. Six different titanium powders were characterized. Equal-magnification scanning electron micrographs of the six powders are presented in Fig. 1. Carbon blacks were supplied by Cabot; their characteristics and impurity levels are shown in Table II. All of the carbon blacks used in this study were amorphous. Two parameters unique to the characterization of carbon blacks are the n-dibutyl phthalate absorption number (DBP) and the tinting strength index (tint index). The DBP is a measurement of the void volume associated with carbon-black aggregates as determined by the adsorption of n-dibutyl phthalate oil ($cm^3/100$ g) using an adsorptometer. It is directly related to its structure. The degree of structure or connectedness increases as the DBP increases. The tint index is inversely proportional to the aggregate size of the carbon black.

At comparatively low magnifications, it is difficult to contrast the scanning electron microscopy (SEM) micrographs of the carbon blacks. Three of the Monarch reactants, however, do differ chemically from the other powders. The chemical characteristics of the two classes of Monarch carbon blacks, along with the Regal carbon black, are presented in Table II.

* *Present address*: Synergetic Materials, Inc., Auburn, CA, 95604 USA.

0022–2461

TABLE I Characteristics of titanium powders

Powder characteristics	Powder source and designation					
	Alfa 00724	Ventron Grade-Z	Micron Ti-020	NMI CPTi2	Atlantic-325	Alfa 99883
Size range (μm)	5–45	2–24	10–203	10–256	2–38	1–68
Mean (μm)	27	12	34	82	20	14
Density ($kg\,m^{-3}$)	4460	4430	4450	4490	4270	4440
Surface area ($m^{-2}\,kg^{-1}$)	300	1900	400	900	4700	700
Analysis (wt %)						
C	0.07	0.28	0.01	0.03	0.19	0.21
H	0.20	0.22	0.16	0.03	0.44	0.18
N	0.05	0.91	0.01	0.02	nd[a]	0.02
O	0.21	0.86	0.17	0.41	3.29	0.83
Zr	nd[a]	0.33	nd[a]	nd[a]	0.32	> 0.50
Al	nd[a]	0.10	nil[b]	nil[b]	0.10	0.01
Ca	0.01	0.02	0.004	nd[a]	0.30	0.01
Fe	nil[b]	nd[a]	0.02	0.17	0.01	nd[a]

[a] Nd: none detected; [b]nil: < 0.0005 wt %

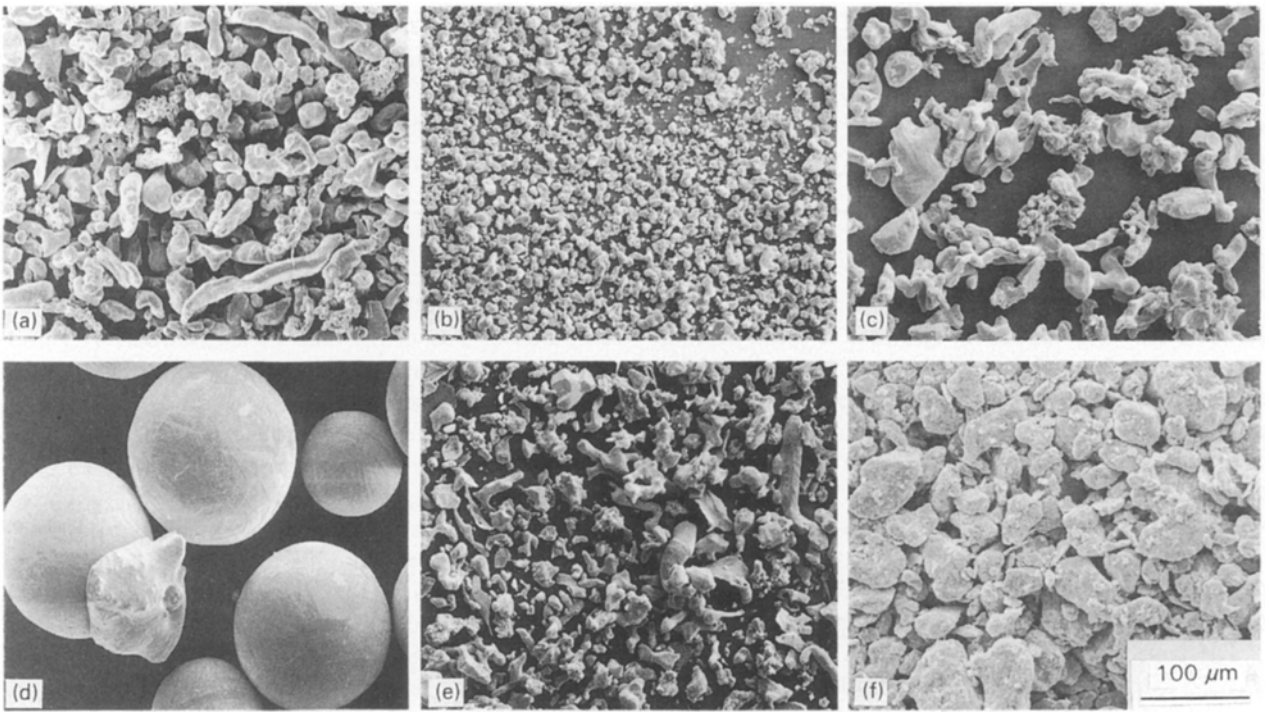

Figure 1 SEM micrographs of titanium powders: (a) Alfa 00724, (b) Ventron Grade-Z, (c) Micron Ti-020, (d) NMI CPTi2, (e) Atlantic-325, and (f) Alfa 99883.

Of the seven graphites used in this study, only one was characterized in this work, the Alfa 00641. This is a natural crystalline-flake graphite (NCFG) with a surface area of 8300 $m^3\,kg^{-1}$ and a PSD (particle size distribution) as follows: 50% ≤ 25 μm, 75% ≤ 50 μm, 90% ≤ 60 μm, 100% ≤ 80 μm. Qualitative XRD analysis showed the material to be mostly type-4H [2] with a trace of type-6R [3] structure. This material has an unusually high measured specific gravity of 2400 $kg\,m^{-3}$ (the theoretical maxima for both the 4H and 6R structures is 2280 $kg\,m^{-3}$). Chemical analyses revealed a purer powder than the carbon blacks: 97.8 wt % C, 0.93 wt % O, 0.06 wt % N, and 0.02 wt % H. Emission spectroscopy indicated the presence of 0.02 wt % Al, 0.01 wt % Si, 0.01 wt % Fe, and ≤ 0.0143 wt % other impurities. SEM observations of this material showed a plate-like morphology. Electron spectroscopy for chemical analysis (ESCA) indicated the powder's surface was mostly carbon (> 95%) with low levels of elemental oxygen (1.6%) and elemental sulphur (0.7%).

Six other graphites were used to produce TiC products. Of the seven graphite powders used, four different types were recognized: synthetic graphite (SG), high-purity synthetic graphite (HPSG), natural crystalline-vein graphite (NCVG), and natural crystalline-

TABLE II Physical characteristics of carbon blacks

	Powder designation									
			Monarch (LVCB[a])					Monarch (HVCB[b])		
	120[c]	250R	700	800	880	900	1000	1100	1300	1400
Density (kg m^{-3})	–	1880	1930	1920	1930	1970	1970	2050	2040	2020
Surface area (m^2 kg^{-1})	25000	66000	246000	230000	252000	257000	250000	400000	547000	586000
Average particle size (nm)	75	35	18	17	16	15	14	16	13	13
DBP no[d] (cm^3/100 g)	72	46	122	74	112	70	65	105	100	90
Tint index[e]	58	95	118	120	122	120	115	116	100	100
Analysis (wt %)										
C	–	96.7	91.7–94.1					82.4–85.2		
H	–	0.17	0.19–0.36					0.65–0.80		
N	–	0.15	0.68–0.96					0.79–0.99		
O	–	0.88	3.3–5.2					11.3–13.7		
Na	–	0.01	0.003–0.06					> 0.5 (1300)		
K	–	nd[f]	> 0.5 (900, 1100)					0.1(1400)		

[a] LVCB: low-volatile-content carbon black.
[b] HVCB: high-volatile-content carbon black.
[c] Vendor supplied data.
[d] Volume of n-dibutyl phthalate oil adsorbed per 100 g.
[e] Relative diffuse reflectance (ZnO paste).
[f] nd: not detected; all other impurities less 0.06 wt %.

TABLE III Characteristics of graphite and carbon powders (Chemistry data is in wt %)

	LVCB	HVCB	CPC (#9 & coke fines)	DCPC (9035)	SG (5035, 5039, 450)	HPSG (5535, 5539)	NCVG (4735)	NCFG (00641)
Carbon (min.)	91.7	82.4	99.2	99.9	99.0	99.8	99.1	99.5
Ash (max.)	0.7	2.1	0.8	0.1	0.8	0.2	0.9	0.5
Sulphur (max.)	1.6	0.8	1.8	< 0.02	0.05	0.02	nil[a]	nil[a]
Volatile (max.)	2.0	9.5	1.0	0.1	0.37	0.01	0.2	0.08
Moisture (max.)	4.7	7.0	0.1	nil[a]	0.12	nil[a]	0.09	0.2
Structure	Am[b]	Am[b]	Am[b]	P Gr[c]	Gr[d]	Gr	Gr	Gr
Density (kg m^{-3})	1940	2040	1820	2170	2280	2280	2280	2400
Surface area (m^2 kg^{-1})	250000	500000	< 10000	< 10000	< 10000	< 10000	< 10000	< 10000

[a] nil: negligible; [b] Am: amorphous; [c] PGr: partially graphitized; [d] Gr: Graphitic.

flake graphite (NCFG). Two types of SG were used in this study: regular SG (Superior 5035, 5039, and Ashbury Micro 450) and HPSG (Superior 5535 and 5539). The chemical analysis of the graphites is given in Table III.

Three coke powders were used to fabricate TiC products (Superior Coke Fines, Superior #9, and Superior 9035). Two types of coke were studied: calcined petroleum coke (CPC) and desulphurized calcined petroleum coke (DCPC). The chemical analysis of these cokes is given in Table III. This table illustrates the wide range of carbon contents, impurity/volatile concentrations, and atomic structures available. These, along with the different particle sizes, will offer a range of parametric variables to form a basis of comparison for the results of this study.

2.2. Sample preparation and green-density measurements

Mixtures of titanium and carbon or titanium and graphite powders were proportionally weighed to produce stoichiometric $TiC_{1.0}$. The total sample charge was approximately 8.0 g. After weighing, the powders were uniaxially cold pressed in a 2.54 cm (1 inch) steel die with free-moving steel punches. Prior to pressing, the reactants were mixed in 10–50 ml of methanol by an ultrasonic probe at 75 W for 4–5 min. The mixture was then vacuum filtered, dried, and pressed. The applied uniaxial pressure was maintained at ~ 35 MPa for several minutes before the green part was removed. Some compacts with very coarse carbons or graphites required the use of a binder. In that case, polyethylene glycol (PEG) was added to the methanol prior to the introduction of the reactant powders and ultrasonic mixing. Binder additions ranged between 10–25 wt % of the methanol–binder solution.

Green densities of cold-pressed compacts were determined using bulk-density calculations based on dry-sample weight and volume (diameter and thickness) measurements. The error associated with this

technique is ± 0.5% in the reported relative density. Green densities were not measured on samples containing binder as it was difficult to determine the volume of binder retained by these samples.

2.3. Sample conditioning, ignition, and synthesis

Prepared green compacts were outgassed, ignited, and synthesized in a temperature-controlled-combustion assembly housed in a glove box. Pre-ignition outgassing was accomplished by heating each sample to 1133 K (860 °C) for 1 h under a vacuum of 3–8 Pa using a 0.25 mm tantalum heating element, which was placed around the inside of a cylindrical quartz sleeve that was slotted to accommodate thermal expansion and contraction. This has been shown to be the optimum treatment [4]. Each sample was placed on its side on top of a graphite pedestal located in the centre of the heating-element assembly. The sample and complete assembly were then surrounded by a kaolin fibrous insulation blanket. The standard heating rate for thermal–vacuum treatments was 25 K min^{-1}. When the binder (PEG) was present, the rate was reduced to 10 K min^{-1} on passing through 573–703 K (300–430 °C). This range was selected on the basis of thermogravimetric analysis (TGA) and differential thermal analysis (DTA) results for the Ti + C + PEG system.

After outgassing, ignition was accomplished by heating the uppermost portion of the sample using a tungsten coil which was placed ~ 0.3 cm above the sample. Ignition and synthesis were performed under a vacuum of 3–8 Pa. This was selected over the use of an inert atmosphere (e.g. argon) to reduce possible oxygen contamination from commercially available inert gases. The presence of oxygen in the environment has been shown to influence the kinetics of combustion of TiC, resulting in reduced rates of synthesis and lower conversion efficiencies [5].

The sample temperature was monitored by a calibrated chromel–alumel thermocouple located in the base of the graphite pedestal. Calibration was first performed using another chromel–alumel thermocouple which was in actual contact with the Ti + C sample and the two outputs were compared and charted for future reference. Subsequent experiments were performed with only the thermocouple in the pedestal.

3. Results and discussion

3.1. Green density of uncombusted samples

The objective of the powder consolidation study was to understand how the characteristics of the different powder types influence the compaction process under uniaxial pressure. Uniaxial cold pressing was used to consolidate the titanium–carbon and titanium–graphite powder mixtures. In comparing the pressing characteristics of the different titanium powders, the Cabot Monarch 900 carbon black was chosen as the standard carbon. Comparisons involving all of the carbon and graphite powders were made using the Micron Ti-020 as the standard titanium. The theoretical densities of the starting constituents strongly influence the calculated relative green densities of the Ti + C compacts. For example, by changing from an amorphous-carbon-black reactant to a crystalline-graphite reactant (an increase of 18% in theoretical particle density), the true density (i.e. with porosity) of the green-reactant mixture using the same titanium (theoretical density = 4460 kg m^{-3}) to obtain a 1 : 1 molar ratio of Ti : C will increase by 6%. All density calculations are based on the molar amount of reactants required to produce stoichiometric $TiC_{1.0}$. Consequently, density results are presented as a relative percentage of theoretical. This normalizes the data and negates the influence of starting-powder-specific-gravity fluctuations in the results.

On a particle–particle scale, two processes of compaction can be distinguished involving three stages and three basic mechanisms [6]. The two processes are differentiated by whether large or small voids are to be filled. In the initial stages of compression, when large voids are to be filled, the process of particle or aggregate rearrangement dominates. In the next stage, the smaller voids must be filled by the fragmentation of larger particles or aggregates. Finally, plastic flow of particles completes the process.

The effect of different titanium reactants on the pre-ignition compact density is presented in Fig. 2. Different titanium powders resulted in green densities in the range 2070–2390 kg m^{-3}. The results of Fig. 2 and the data listed in Table I indicate that the green density increases as titanium-powder size increases. The titanium powders producing the lowest green densities also had the highest surface areas (Ventron Grade-Z and Atlantic-325). These higher surface areas indicate an increased surface roughness and degree of irregularity which inhibit particle sliding and rearrangement mechanisms. The highest green densities were obtained with very large spherical titanium powders, ~ 82 μm average diameter (Nuclear Metals (NMI) CPTi2). As indicated in Table I, this titanium is the purest. This combined with its large size (less surface to influence re-arrangement mechanisms) will offer more ductility and consequently better plastic flow. Because all the titanium powders were mixed with

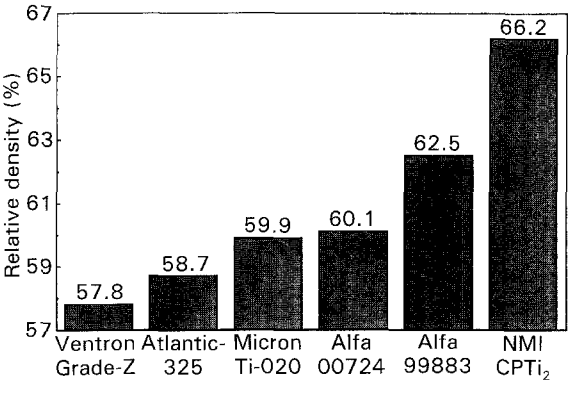

Figure 2 Green densities of uncombusted Ti + C compacts as a function of titanium powder (samples pressed at ~ 35 MPa using Cabot Monarch 900 carbon black).

a small-aggregate, low-structure carbon black (Monarch 900), the fragmentation process should be similar regardless of the titanium used. Hence, this mechanism should not influence the results of Fig. 2. It should be noted that the green densities of the Micron Ti-020 and the Alfa 00724 were almost identical (59.9% and 60.1%, respectively). The authors believe that these are the same powders made available by two suppliers.

Next, the small-aggregate carbon blacks were compared to determine their effect on compact density. The results, plotted against vendor-supplied DBP values, are presented in Fig. 3. The results of the Regal 250R and Monarch 120 carbon blacks are not shown in Fig. 3. This is because they are larger aggregate bodies and although they follow the trend discussed here their compaction mechanisms should be more applicable to the other carbons and graphites of this study. Consequently, they will be discussed in a later section. Fig. 3 clearly shows the strong effect of carbon-black structure on the packing density of the Ti + C compact. The higher the structure, as indicated by the DBP, the lower the reactant-body green density. This is intuitively obvious, as a higher degree of structure indicates greater connectedness within each aggregate. This imparts a greater structural integrity (strength) to the aggregate which in turn makes the fragmentation process more difficult during compaction. Soviet investigators have examined the influence of different carbon blacks on the synthesis of TiC by self-propagating reactions, using the DBP as a parameter [7]. Their work, however, failed to recognize the significance of the role played by the degree of structure in the pre-ignition compact density, a role which has been shown to be directly related to combustion-synthesis mechanisms and product microstructure [8].

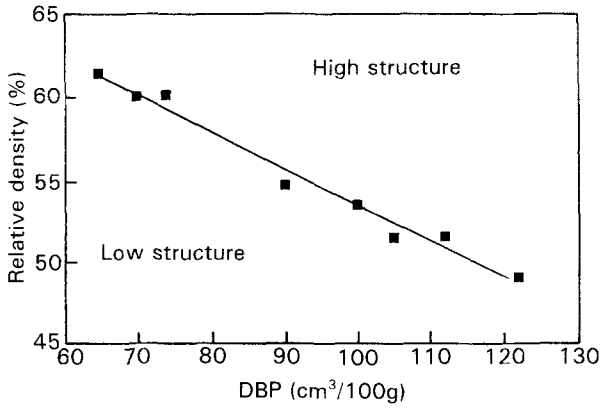

Figure 3 Effect of structure (DBP) of carbon blacks on the density of uncombusted Ti + C compacts (Ti powder: Micron Ti-020; uniaxial pressure: ~ 35 MPa).

Fig. 4 shows the effect of using different carbon reactants on the green density of the Ti + C compacts while holding the titanium reactant constant (Micron Ti-020). Fig. 4 indicates that large-aggregate carbon blacks pack more tightly than the natural graphites. The natural graphites, in turn, pack better than the SGs and small-aggregate carbon blacks of low-structure. The lowest packing densities are obtained with small-aggregate carbon blacks possessing high structure. Within this latter category, HVCBs (Monarch 1300, 1400) appear to display better packing behaviour than the LVCBs (Monarch 700, 880, 1000). This is probably due to the HVCBs chemically treated surface which produces a higher surface area and consequently reduces the structural integrity of the aggregate, allowing it to fragment more easily during the pressing process. This is in contrast to the previously mentioned effect of increased surface area on the titanium particles, where higher surface area results in increased surface roughness which inhibits rearrangement.

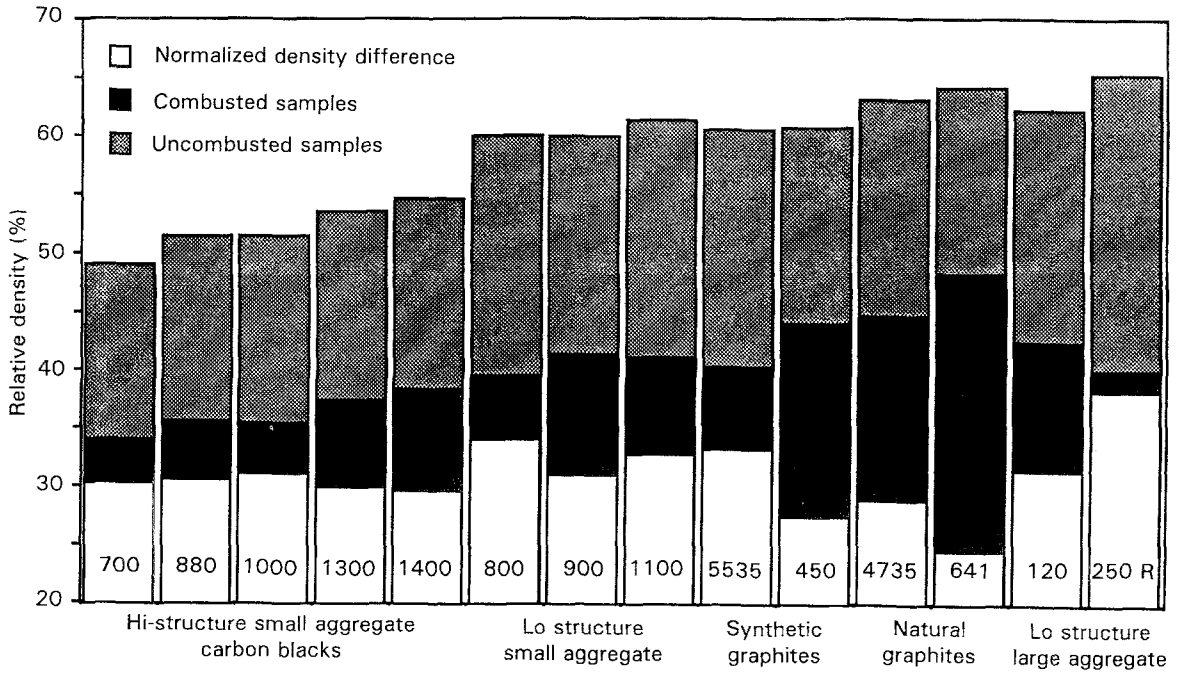

Figure 4 The densities of combusted and uncombusted Ti + C compacts for a variety of carbon blacks and graphites (Ti powder: Micron Ti-020, numbers on the bars refer to manufacturers' designation).

When a compact of a 100% Ti (Micron Ti-020) was cold pressed at ~ 35 MPa, the resulting density was 62.5% of the theoretical value. With reference to the results of Fig. 4, it is interesting to note that the addition of most of the carbon and graphite powders resulted in a reduction of the density of the green compacts. Only in the case of the Alfa 00641 graphite and the Regal 250R carbon black did the addition of the other reactant increase the density of the mixture.

The primary problem associated with the uniaxial pressing of powder mixtures relates to the geometry of the pressure distribution. Axial forces applied to powder compacts constrained to a die cavity result in radial forces on the compact. These radial forces, with their magnitude largely dependent on the plasticity of the powders, result in stress-concentration gradients within the compact [9]. The harder and more elastic reactant particles tend to form interlocking bridges in the regions of high stress concentrations which inhibit further particle rearrangement, fragmentation, and plastic flow. This results in non-uniform green-density distributions. It has also been shown that the porosity of a compact, comprised of spherical powders, located adjacent to the die wall can be 15–20% higher than in the central portion of the die cavity [10].

3.2. Density and microstructure of combusted samples

An examination was made of the microstructures of combusted samples of the standard titanium (Micron Ti-020) with small-aggregate, high-structure carbon blacks (Monarch 700, 880, 1000), with small-aggregate, low-structure carbon blacks (Monarch 800, 900, 1100), and with HVCBs, which are intermediate to the others in structure (Monarch 1300, 1400). Representative microstructures of these three general groups are shown in Fig. 5a–c. It should be pointed out that in these micrographs the white phase is TiC, the grey regions are the mounting epoxy, and the black regions are pores. The higher surface area associated with HVCBs (Fig. 5c) can be compared to the lower surface area LVCBs with high (Fig. 5a) and low (Fig. 5b) structure. These high-magnification views reveal that a finer network structure is obtained with the high-surface-area carbon blacks. The finer network structure exhibits product cavity walls between 1–10 μm thick, whereas the coarser networks display cavity walls between 5–20 μm thick.

As stated earlier, the structure of carbon black is quantitatively described by the DBP. To show the effect of structure, the DBP number for the samples presented in Fig. 5a–c is plotted against the relative density of the uncombusted and combusted samples in Fig. 6a. Also plotted in Fig. 6a is a normalized difference between these densities as a function of DBP number. The normalized difference is calculated by dividing the difference between green and combusted densities by the green density for that sample. Fig. 6a shows the influence of structure on product density. The use of carbon blacks with lower structure resulted in slightly higher product densities. Carbon blacks with higher structure and coarser networks resulted in smaller density changes during synthesis. Fig. 6a also shows that the use of carbon blacks with higher surface areas (open data points) does not affect the combusted product density as much as it affects the morphology of the network. The correlation between green-compact density and product density indicates that green-compact density is, expectedly, a key parameter in controlling product density. This is clearly shown in Fig. 6b where the same data are plotted as the density of the combusted product versus the density of the green compact.

Next, the results of varying the titanium powder while using the Monarch 900 carbon black as a standard are examined. Microstructural comparisons of the combusted samples are presented in Fig. 7a–d. It is clear from Fig. 7 that coarser microstructures were obtained with the Micron and the Alfa (99883) Ti

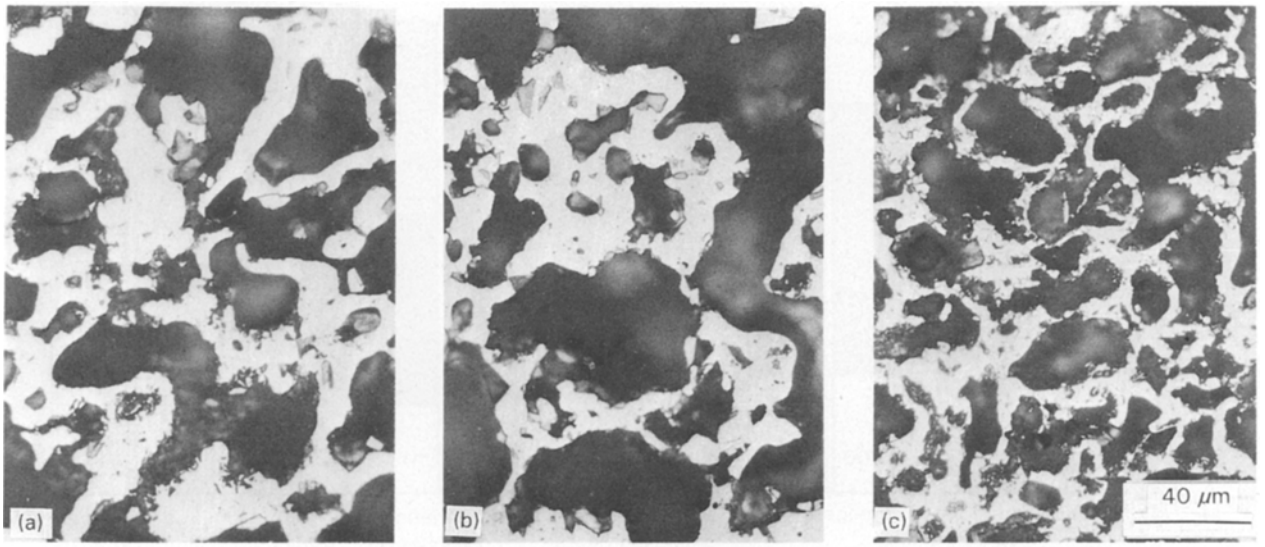

Figure 5 Microstructures of combusted TiC made with three types of carbon blacks (Ti powder: Micron Ti-020): (a) Monarch 880 (b), Monarch 900, and (c) Monarch 1300.

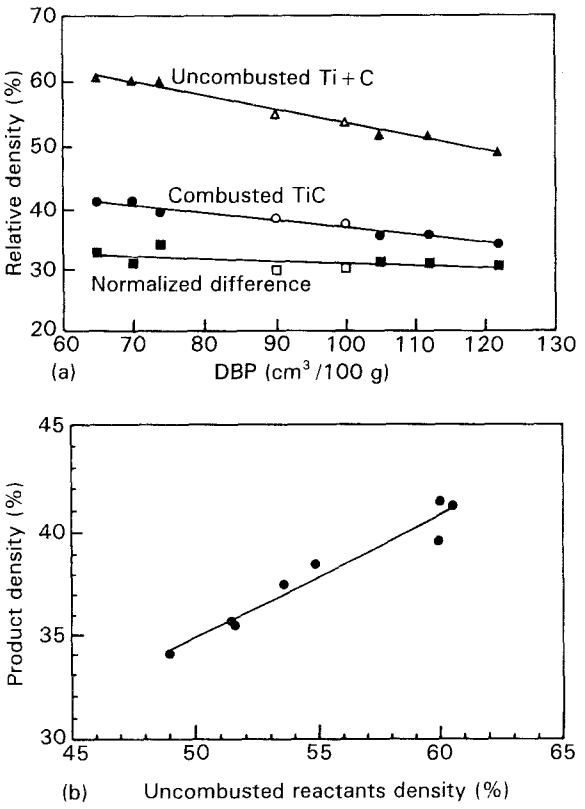

Figure 6 (a) The effect of carbon-black structure on the relative densities of combusted and uncombusted Ti + C compacts. (△ ○ □) HVCB, and (▲ ● ■) LVCB. (b) The relationship between densities of uncombusted and combusted samples (Ti powder: Micron Ti-020, small-aggregate carbon blacks except Monarch M120).

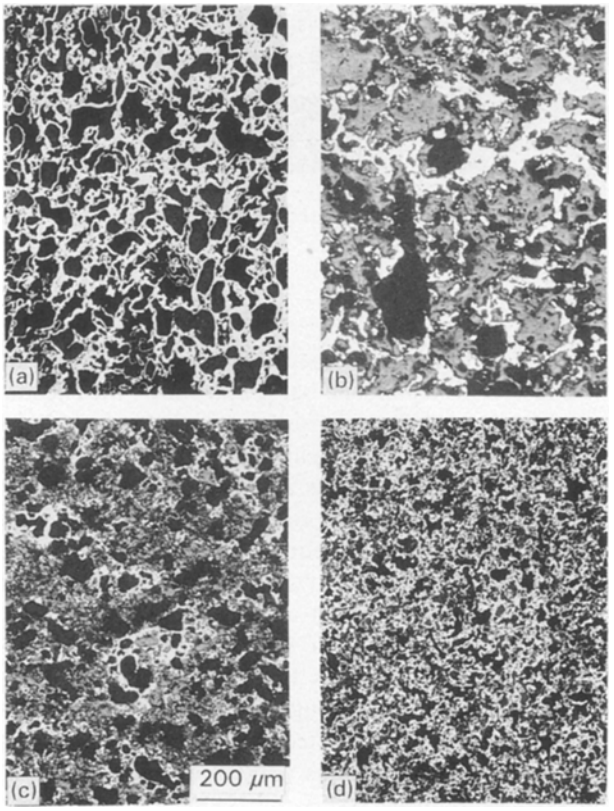

Figure 7 The microstructures of combusted TiC made with Monarch 900 carbon black and four types of titanium powders: (a) Alfa 99883, (b) Micron Ti-020, (c) Atlantic-325, and (d) Ventron Grade-Z.

powders and that the finer structures were obtained with the Ventron and Atlantic powders. This is consistent with the differences in the starting Ti powders, as shown in Fig. 1. The Nuclear Metals CPTi2 titanium did not support combustion at all.

Fig. 8 shows the relative green-compact and synthesized-product densities, along with their differences for each of the titanium powders supporting combustion. It is interesting to note that green-compact densities showed no significant variation, while the combusted-product densities increased from 34.1 to 41.4%. Attempts to correlate the chemical and physical parameters of the titanium powders (Table I) with these results were difficult because of the absence of clear trends.

Finally, the effect of using different types of carbon and graphite was examined using the standard titanium. The large-aggregate carbon blacks are compared in Fig. 9.; the Monarch 120 has a denser and more reticulated structure than the Regal 250R. Large-aggregate carbon blacks produced higher product densities than small-aggregate carbon blacks. It is interesting to note that the Regal 250R had a higher green density than the Monarch 120, but the latter produced a higher-density product. This is noteworthy in that the Monarch 120 has a larger particle size (75 nm) than the Regal 250R (35 nm). The typical particle size for the small-aggregate materials is 13–18 nm (Table II). Thus, to a lesser extent, the aggregate particle size also influences product microstructure: larger particles producing coarser and denser networks, and vice versa.

Fig. 10 shows the microstructures of products made with regular (CPCs) and desulphurized (DCPCs) calcined petroleum cokes. Due to the very coarse nature of the CPCs and the high resiliency of the DCPCs, a binder was required to fabricate stable pre-ignition compacts. Consequently, the product densities were lower than if a binder had not been used. Despite this, striking differences in network morphology are realized, as shown in Fig. 10. It is notable that the very coarse (− 65 mesh) coke fines produced a much coarser assemblage than did the finer (− 200 mesh) #9 amorphous carbon, which in turn produced a coarser network than did the finer (− 325 mesh) desulphurized coke. This follows the particle-size-to-structure relationship previously realized on a nanoscale with the carbon blacks.

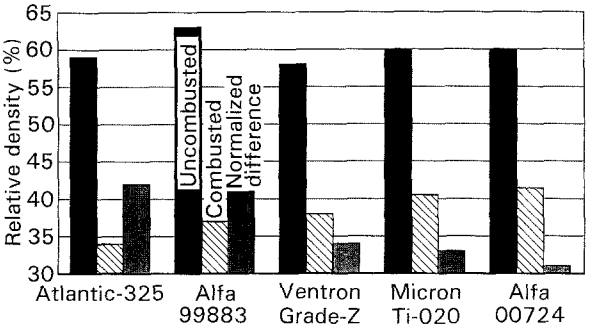

Figure 8 The effect of titanium powder on the densities of combusted and uncombusted Ti + C compacts (carbon black: Monarch 900).

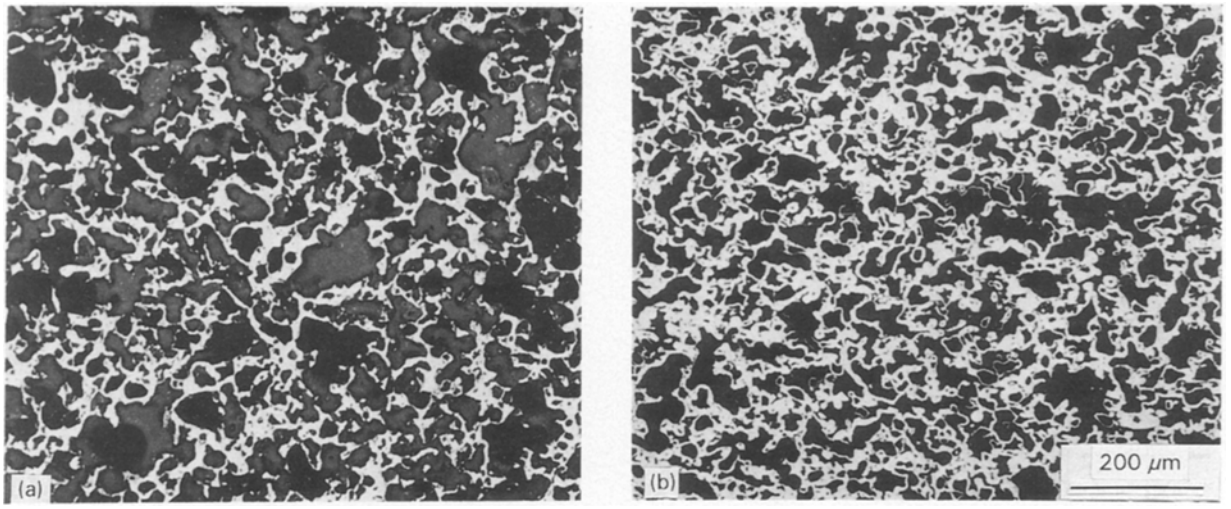

Figure 9 Microstructures of combusted TiC made with low-structure, large-aggregate carbon blacks (Ti powder: Micron Ti-020) : (a) Regal 250R, and (b) Monarch 120.

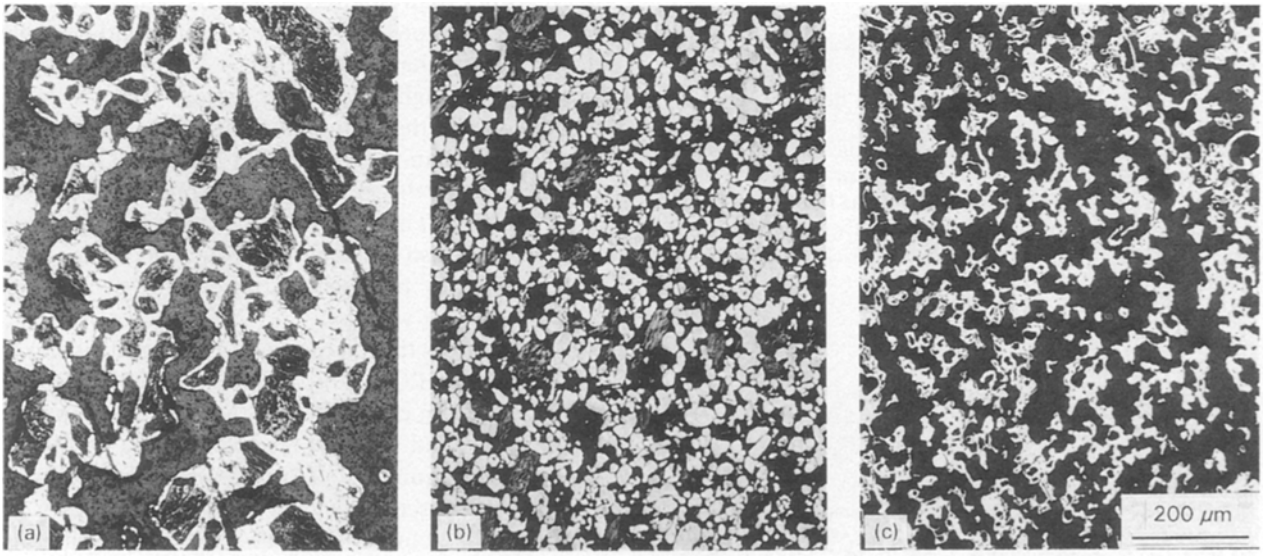

Figure 10 Microstructures of combusted TiC made with different cokes (Ti powder: Micron Ti-020). (a) Superior coke fines, (b) # 9, and (c) 9035.

The microstructures of products fabricated from regular (SGs) and high-purity (HPSGs) synthetic graphites were also examined. Structure-assemblage differences resulting from different particle-size graphites are small in comparison to those for carbon. An example of the microstructure of a product is shown in Fig. 11a for the HPSG. The microstructures of products synthesized using natural graphites are illustrated in Fig. 11b and c. The 00641 NCFG and the 4735 NCVG are both reported as -325 mesh (~ 44 μm) powders, yet a substantial difference in network morphology is evident. This difference, we believe, is caused by differences in combusted sample densities (see Fig. 4). The NCVG sample, with a lower density, cooled at a slower rate resulting in a coarser microstructure. This aspect of the synthesis of TiC will be discussed in a subsequent paper [8].

Relative-density data for the self-propagating high-temperature synthesis (SHS) products, green pre-ignition compacts, and their differences are presented in Fig. 4. This composite bar graph shows the effect of varying the carbon and graphite type when no binder is used. As previously mentioned, a binder was used with some of the carbons and graphites. These data will not correlate with results for products made without binder and consequently these products were not included in Fig. 4. It should also be noted that product densities are not available for two samples: the 5539 (HPSG) which would not support combustion, and the #9 (CPC) which only partially reacted, leaving only enough material for microstructural examination. Repeated attempts to ignite identical reactant compositions containing the #9 (CPC) powder were unsuccessful.

To simplify the results and to improve identification of product density and density difference as they relate to a particular type of carbon or graphite, the data of each category were averaged and they are listed in

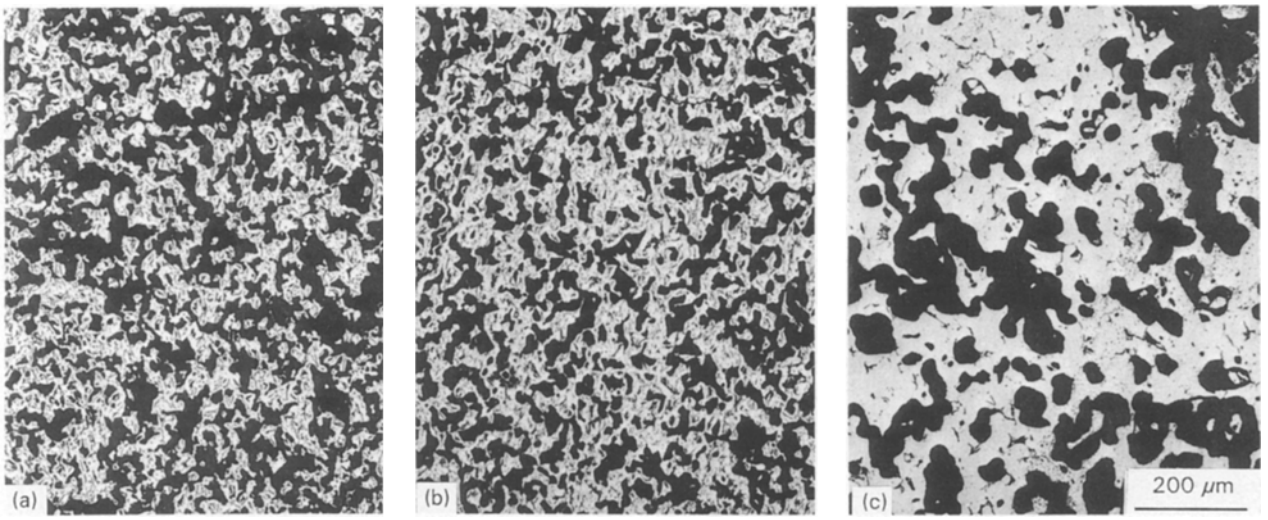

Figure 11 Microstructures of combusted TiC made with different graphites (Ti powder: Micron Ti-020): (a) Superior 5535, (b) Alfa 00641, and (c) Superior 4735.

TABLE IV Density data of combusted and uncombusted Ti + C compacts (Ti powder: Micron Ti-020)

Carbon and graphite type	Product density (%)	Density difference[a] (%)
High structure, small aggregate	36.3	30.4
Low structure, small aggregate	40.7	32.7
Low structure, large aggregate	41.4	35.1
Synthetic graphite	42.3	30.4
Natural graphite	46.6	26.8

[a] The density difference between combusted and green compacts.

Table IV. Table IV indicates that natural graphites produced the highest product density while small-aggregate, high-structure carbon blacks produced the lowest. The range is 36.3–46.6% (1790–2300 kg m^{-3}). Low-structure carbon blacks resulted in comparable product densities regardless of their aggregate size. This is in contrast to the data of Fig. 4, where low-structure, large-aggregate carbon blacks resulted in very high green densities. This point is emphasized in Table IV where the highest volume change is also associated with these materials. The SGs had only a slightly increased product density relative to low-structure carbon blacks. However, they did exhibit a much smaller volume change.

According to Table IV, both carbon blacks and graphites produce products with density differences above the theoretical molar volume change (24.4%) for TiC. This means that increases in volume occur during synthesis regardless of the type of carbon or graphite. However, the smaller the volume change, the stronger the correlation between the green density and product density. An interesting observation is that the small-aggregate, high-structure carbon blacks, which resulted in the lowest green and product densities, displayed the smallest volume change of all carbon blacks. The natural graphites, which resulted in very high green densities and the highest product densities, displayed the overall smallest volume change. The explanation for this apparent discrepancy is in the degree of structure itself. High-structure carbon blacks possess a high degree of connectedness as indicated by their very high DBP values (Table II). Natural graphites, however, have the ability to pack tightly into the tortuosities of the titanium particles. This, combined with their relatively low resiliency, allows for an intimate contact arrangement between reactants that simulates a very high degree of structure within the pre-ignition compact. The only difference between the structure of the carbon blacks and the structure of natural graphites is in their size scale (nanometres versus micrometres). Experimental verification of this structure effect in titanium + carbon black SHS reactions has been reported [7]. The results showed that high-structure carbon blacks had faster combustion velocities than low-structure carbon blacks.

A relationship between carbon particle size and the TiC-product grain size, as observed in this study, has been suggested in some papers [11, 12] and discounted in others [13, 14]. Furthermore, it is observed (see Table III) that a reactant-surface-area-versus-network-morphology relationship also exists. The very high surface areas ($\sim 5 \times 10^5$ m^2 kg^{-1}) of the HVCBs resulted in finer networks than those obtained when low surface area blacks were used. In a previous work, attempts to correlate the surface area of carbon blacks to the TiC microstructure did not show this relationship because, we believe, of the limited number of carbon blacks evaluated [14].

In one set of experiments a mixture of the standard Ti and the Regal 250R carbon black was uniaxially pressed at $\sim$ 138 MPa and compared to a mixture pressed at the standard condition, $\sim$ 35 MPa. The green densities of the low-pressure and high-pressure compacts were 65.3% and 74.9%, respectively and the SHS product densities were 40.2% and 43.0%, respectively. This is not too significant a difference considering the large green density increase of 9.6%.

Under higher magnification, the -200 mesh ($\sim 74\,\mu m$) #9 morphology does not resemble the continuous reticulated grains on the -65 mesh ($\sim 230\,\mu m$) coke fines typically found in the SHS products of this study. Instead, it has the appearance of individual TiC grains that are partially sintered together. The grain morphology of the two CPCs differs considerably and is believed to be the consequence of differences in ash content in the two cokes. The coarser CPC (coke fines) compacts were easily ignited, whereas ignition was difficult with the finer CPC (#9), if not impossible. This type of non-ignition behaviour is typically found to occur in coarser, rather than finer, grades of reactants. At present, there is no explanation for the anomalous behaviour of these cokes.

High-magnification views of the products made from the SGs show a weak relationship between the TiC network morphology and the graphite particle size. The TiC product assemblage becoming only slightly coarser as the reported graphite size increases by orders of magnitude (from 0.6 to 5 to 44 μm for the 450, 5039, and 5535 graphites, respectively). This is in contrast to the same relationship for carbon blacks, where substantial changes in TiC product morphology occur within a single order-of-magnitude range of particle sizes (13–75 nm). The coarsest network assemblages are realized with the natural graphites. Product-cell-wall thicknesses in excess of 100 μm are possible with the 4735 NCVG. Although the 00641 NCFG produced a finer network than the NCVG, it resulted in a 1.0% higher green density and a 3.6% higher product density. A more subtle variation occurs in the grain character of some of the products. This behaviour was first observed by Halverson *et al.* [15] in an earlier study where carbon blacks and graphites were mixed together prior to being combined with the titanium reactant. The results indicated a grain texture changing from smooth to rough as the graphite-to-carbon reactant ratio was increased. The present study presents similar findings, but also offers a possible explanation to this observation.

Re-examination, at higher magnification, of the microstructures for the HPSG 5535 (Fig. 12a) and the coarse CPC coke fines (Fig. 12b) reveals the appearance of a cored grain texture. Such a microstructure was not observed in the regular SGs the finer CPCs, the natural graphites, and the carbon blacks which appeared to have the more typically smooth grain texture commonly associated with SHS microstructures. A unique feature of this coring effect is that it was only noticed in Ti + C systems in which the carbon or graphite powders possess a very low ash content. According to vendor specifications, the CPC (coke fines) and the HPSG (5535) have average ash contents of ≤ 0.3 wt %. Samples containing these materials resulted in the only two microstructures that displayed cored grain textures. All other carbon and graphite products, with higher ash contents, had smooth grain textures. The explanation of this phenomenon is probably linked to the fact that the ash is made up of oxides like SiO_2, Al_2O_3, and Fe_2O_3.

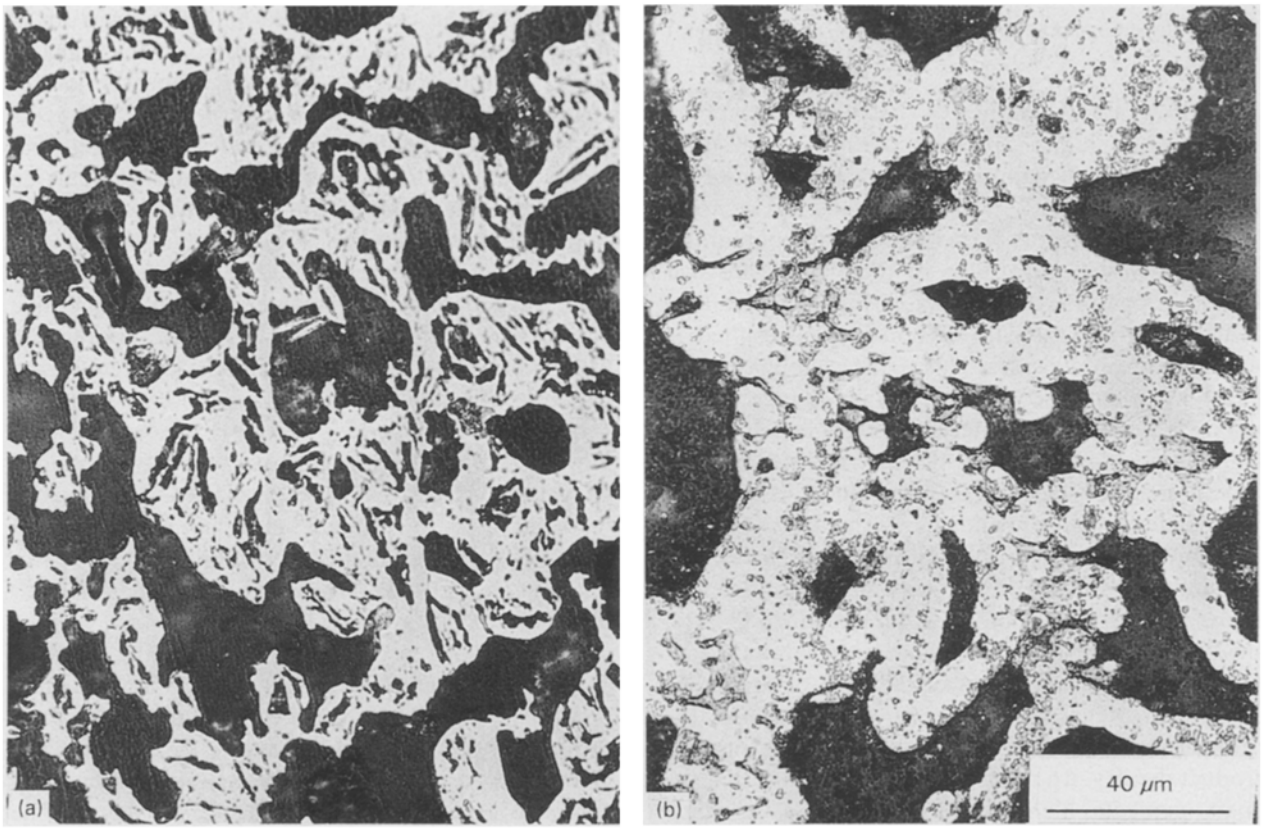

Figure 12 Microstructures of combusted TiC made with HPSG and regular CPC (Ti powder: Micron Ti-020). (a) Superior 5535, and (b) Superior coke fines.

Although the tendency is toward purification during synthesis, such oxides are relatively non-volatile and their presence cannot be discounted. Titanium carbide can dissolve considerable amounts of oxygen by substitution for carbon [16]. This occurs readily when the lattice is not saturated (as in non-stoichiometric TiC). The result is an oxycarbide which can be considered as a complex solid solution between TiC and the residual metal oxides of the ash. Because very small additions of carbon and oxygen to titanium result in eutectics [16], the formation of ternary and higher order eutectics is also feasible. In addition, the melting points of the oxides typically contained in carbon and graphite ash – e.g. SiO_2 (1995 K), Al_2O_3 (2323 K), and Fe_2O_3 (1867 K) – are lower than the melting point of TiC (3423 K) [17]. This implies that during the final stages of synthesis, structural transformations that are occurring as the product cools will be aided by the presence of liquid phases. This will most likely be in the form of enhancing liquid-phase sintering on a local scale, although densification will be negligible due to the large volume expansion that occurs during the synthesis of TiC. In systems with a very low ash content, cooling through the TiC solidus may be faster due to the absence of low melting or eutectic phases. This phenomenon may occur fast enough to impart a non-equilibrium microstructure to the grains [18] or at least a lesser degree of structuralization.

4. Conclusion

The influence of reactant characteristics on the amount of porosity and microstructural morphology in combustion-synthesized porous ceramic products was investigated using titanium carbide as an experimental system. The size of the titanium particles does not greatly influence final product density. It does, however, affect the morphology of the reticulated network in the product with finer particles resulting in finer assemblages and vice versa.

Carbon-black structure strongly influences the compaction and consolidation of pre-ignition compacts. Low-structure carbon blacks result in higher green densities than high-structure carbon blacks. This is because high-structure carbon blacks are more connected and impart a greater strength to the aggregate which inhibits fragmentation during compaction.

Increasing the applied pressure during compaction can increase the green density of the pre-ignition compact, however, very high green densities have been shown to result in decreased combustion kinetics and incomplete product formation. Consequently, low-pressure consolidation in the neighbourhood of 35–70 Mpa is preferred for the fabrication of uniform porosity products.

The large-aggregate carbon blacks and the natural graphites resulted in higher green densities than the small-aggregate carbon blacks and the SGs. During the Ti + C compaction process with large-aggregate carbon blacks, the ultrasonically disrupted aggregates initially fill the tortuosities of the titanium particles. As the pressure is increased, the aggregates fragment and accommodate the plastic flow of the titanium during the final stages of compaction. With graphite, the platelets also initially fill in and around the irregularities of the titanium particles. The second stage, however, is not one of fragmentation alone but includes platelet sliding due to graphite's low friction coefficient. Also, graphite is softer and more yielding than carbon black, which not only accommodates the final compaction stage where the plastic flow of titanium dominates, but also results in increased titanium–graphite contacts. The SG yielded slightly lower green densities than natural graphites due to their higher purity, which makes them harder and less accommodating.

Combustion - synthesized - porous - TiC - product density is a function of the pre-ignition-compact green density of the Ti + C reactants. For the carbon categories identified in this study (small-aggregate carbon blacks, large-aggregate carbon blacks, and all graphites), product density will generally increase with increasing pre-ignition compact green density. The only exception to this is realized with the large-aggregate carbon blacks, where a higher green density resulted in a lower product density. However, despite this anomaly, the large-aggregate carbon blacks yield higher product densities than small-aggregate carbon blacks. The natural graphites also resulted in higher-density products than the SGs.

The final product density of small-aggregate-carbon-black systems is also a function of structure, where higher densities are obtained with lower-structure carbon blacks. However, the change in density is also greater with the lower-structure blacks, indicating that greater volume expansion occurs with these reactants than with higher-structure carbon blacks.

Carbon or graphite reactant surface area does not influence product density directly. High-surface-area carbon blacks do, however, produce finer network morphologies than lower-surface-area carbon blacks. The PSD mean for a carbon black tends to influence the network morphology in the TiC product. As the PSD mean increases the assemblage becomes coarser. To a lesser extent, the same effect is observed with graphite-containing systems.

Residual ash content, present in some carbon and graphite reactants, can act as a sintering aid and result in product grain size and assemblage-morphology differences compared to materials synthesized with similar reactants containing lower average ash content (≤ 0.3 wt %). Products produced from the lower-ash-content reactants are uniquely characterized by a cored or pitted grain texture, while products from the higher-ash-content reactants characteristically possess smooth and flat grains.

Acknowledgements

Beverly Lum, Greg Bianchini, and the late Donald Kingman are acknowledged for their contributions in the early experimental phase of this study. This work was supported by a grant from the Lawrence Livermore National Laboratory.

References

1. D. C. HALVERSON, PhD dissertation, University of California, Davis, (1990).
2. JCPDS 25-284, Powder Diffraction File: Inorganic Phases (Joint Committee of Powder Diffraction Standards, Swarthmore, PA, 1975).
3. JCPDS 26-1079, *ibid.*, 1976.
4. D. C. HALVERSON, K. H. EWALD, and Z. A. MUNIR, to be published.
5. V. N. BLOSHENKO, V. A. BOKII, and I. P. BOROVINSKAYA, *Combust. Explos. Shock Waves* **21(1)** (1985) 88–92.
6. A. R. COOPER and L. E. EATON, *J. Amer. Ceram. Soc.* **45** (1962) 98.
7. V. M. SHKIRO, I. P. BOROVINSKAYA, and A. G. MERZHANOV, *Sov. Powder Metall. Met. Ceram.* **18** (1979) 684–87.
8. D. C. HALVERSON, K. H. EWALD, Z. A. MUNIR, to be published.
9. R. A. THOMPSON, *Amer. Ceram. Soc. Bull.* **60(2)** (1981) 237–51.
10. R. F. BENENATI and C. B. BROSILOW, *AIChE J.* **8(3)** (1962) 359–61.
11. M. E. MULLINS and E. RILEY, *J. Mater. Res.* **4(2)** (1989) 408–11.
12. R. A. CUTLER, A. V. VIRKAR, and J. B. HOLT, *Ceram. Engng. Sci. Proc.* **6 (7–8)** (1985) 715–28.
13. S. ADACHI, T. WADA, T. MIHARA, Y. MIYAMOTO, M. KOIZUMI, and O. YAMADA, *J. Amer. Ceram. Soc.* **72(5)** (1989) 805–09.
14. J. B. HOLT, *Advanced Ceram* **21** (1987) 301–10.
15. D. C. HALVERSON, Z. A. MUNIR and B. Y. LUM, in "Combustion and Plasma Synthesis of High Temperature Materials", edited by Z. A. Munir and J. B. Holt (VCH, New York, 1990) p. 262.
16. E. K. STORMS, "The Refractory Carbides", edited by J. L. Margrave, (Academic Press, New York, 1976) p. 225.
17. O. KUBASCHEWSKI and C. B. ALCOCK, "Metallurgical Thermochemistry", 5th Edn (Pergamon Press, Oxford, 1979) pp. 276–323.
18. P. GORDON, "Principals of Phase Diagrams in Materials Systems", (R. E. Krieger Publishing Company, 1983), pp. 65–70.

Received 26 February
and accepted 17 November 1992